Nondestructive evaluation of a new hydrolytically degradable and photo-clickable PEG hydrogel for cartilage tissue engineering

Alexander J. Neumann[a], **Timothy Quinn**[b], and **Stephanie J. Bryant**[a,c,d,*]

[a]Department of Chemical and Biological Engineering, University of Colorado, Boulder, CO 80309, USA

[b]Applied Chemicals and Materials Division, National Institute of Standards and Technology, Boulder, CO 80305, USA

[c]BioFrontiers Institute, University of Colorado, Boulder, CO 80309, USA

[d]Materials Science and Engineering Program, University of Colorado, Boulder, CO 80309, USA

Abstract

Photopolymerizable and hydrolytically labile poly(ethylene glycol) (PEG) hydrogels formed from photo-clickable reactions were investigated as cell delivery platforms for cartilage tissue engineering (TE). PEG hydrogels were formed from thiol-norbornene PEG macromers whereby the crosslinks contained caprolactone segments with hydrolytically labile ester linkages. Juvenile bovine chondrocytes encapsulated in the hydrogels were cultured for up to four weeks and assessed biochemically and histologically, using standard destructive assays, and for mechanical and ultrasound properties, as nondestructive assays. Bulk degradation of acellular hydrogels was confirmed by a decrease in compressive modulus and an increase in mass swelling ratio over time. Chondrocytes deposited increasing amounts of sulfated glycosaminoglycans and collagens in the hydrogels with time. Spatially, collagen type II and aggrecan were present in the neotissue with formation of a territorial matrix beginning at day 21. Nondestructive measurements revealed an 8-fold increase in compressive modulus from days 7 to 28, which correlated with total collagen content. Ultrasound measurements revealed changes in the constructs over time, which differed from the mechanical properties, and appeared to correlate with ECM structure and organization shown by immunohistochemical analysis. Overall, non-destructive and destructive measurements show that this new hydrolytically degradable PEG hydrogel is promising for cartilage TE.

Graphical Abstract

---

[*]Corresponding author at: Department of Chemical and Biological Engineering, University of Colorado, Boulder, CO 80309, USA. Tel.: +1 303 735 6714. sbryant@colorado.edu (S.J.Bryant).

Publisher's Disclaimer: This is a PDF file of an unedited manuscript that has been accepted for publication. As a service to our customers we are providing this early version of the manuscript. The manuscript will undergo copyediting, typesetting, and review of the resulting proof before it is published in its final citable form. Please note that during the production process errors may be discovered which could affect the content, and all legal disclaimers that apply to the journal pertain.

Non-destructive measurements capture neo-cartilage matrix (green) evolution in a new photo-clickable and degradable hydrogel with encapsulated cartilage cells
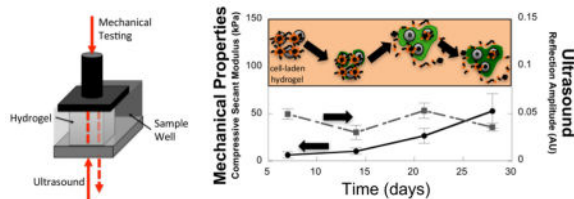
1. Introduction

Hyaline, articular cartilage is the tissue that covers the osseous ends in diarthrodial joints and is responsible for absorbing forces and allowing for a smooth, almost frictionless motion between the articulating surfaces [1]. Once damaged, its intrinsic capacity for repair is low. Cartilage defects that are left untreated can lead to the onset of secondary osteoarthritis [2], which has a high socio-economic burden [3]. Clinically available treatment options for defects in articular cartilage, such as microfracture [4], mosaicplasty [5] and autologous chondrocyte implantation [6], still fail to demonstrate reproducible success. The poor outcome is associated with the formation of a fibrous, mechanically inferior tissue [7]. Matrix assisted autologous chondrocyte implantation, whereby cells are delivered within a three-dimensional (3D) matrix, has the potential to overcome this shortcoming. However, the ideal matrix has yet to be identified.

Poly(ethylene glycol) (PEG) hydrogels have shown promise as a cell encapsulation platform for cartilage tissue engineering (TE) [8–11]. However, the tight mesh of the hydrogel crosslinks, which maintains cells within the 3D hydrogel, impedes diffusion of the cell-secreted extracellular matrix (ECM) molecules and thus inhibits macroscopic tissue growth [12, 13]. The introduction of labile bonds within the crosslinks is therefore necessary to promote tissue growth. However, the challenge is matching the rate of degradation with the rate of neo-tissue synthesis, which is necessary to preserve the mechanical integrity of the material while at the same time, providing adequate space for the deposition of newly synthesized ECM. Degradable hydrogels formed from purely synthetic based chemistries remain a promising approach given the high fidelity and reproducibility of synthetic materials. Previous studies have used PEG hydrogels formed from PEG dimethacrylate monomers containing poly(lactic acid) (PLA) segments to introduce hydrolytically labile esters within each crosslink. These studies have demonstrated that if degradation of the hydrogel occurs too fast, the overall construct mechanical properties drop dramatically with time despite the presence of elaborated ECM molecules [14].

In an effort to identify an improved purely synthetic and degradable PEG hydrogel for cartilage TE, the present study investigated degradable PEG hydrogels synthesized from a thiol-ene photoclickable hydrogel platform [15], but with the introduction of caprolactones. Previous work from our group demonstrated that free-radical polymerization using thiol-norbornene macromers led to a mild encapsulation environment when compared to acrylate macromers due to the nature of the types of radicals formed during encapsulation [8]. This

resulted in a deposition of neo-tissue that more closely resembled hyaline cartilage. In addition, the introduction of ester bonds within the crosslinks offers a strategy to introduce hydrolytic degradation. The rate of hydrogel degradation can be, to some extent, controlled by changing the crosslink density of the material, the chemistry of the ester linkage (e.g., caprolactone) and by changing the number of ester bonds within the crosslink [16–18].

Standard assays, used for assessing cartilaginous tissue production or quantifying the cell number within hydrogel constructs, are typically destructive [19–21]. A method that allows for evaluating the progression of cartilage matrix production *in situ*, without the need to sacrifice the sample would harbor many advantages, such as reducing sample numbers, enabling real time adjustments to the culture conditions, and offering an on-line assessment for clinically, *in vitro* grown engineered cartilage. In the current study, an instrument with combined capabilities of mechanical assessment and ultrasound was investigated as a means for nondestructive evaluation of the hydrogel constructs [22]. Ultrasound measurements of hydrogels, specifically agarose, have been correlated with mechanical properties of the material [23]. In addition, ultrasound measurements of cartilage have been correlated with mechanical properties of the tissue as well as its collagen content [24, 25]. Ultrasound has also been previously demonstrated to show promise when investigating neo-cartilage tissue deposited in synthetic hydrogels [22, 26].

The overall goal of the present study was to assess whether non-destructive measurements could be used to track the progress of neo-tissue development in a modern degradable scaffold system and perhaps then be useful as a quality control variables in the *ex-vivo* manufacture of engineered tissue. A new, photo-clickable and hydrolytically degradable PEG hydrogel formed from thiol-norbornene macromers containing caprolactone segments for cartilage TE was used for the assessment. Hydrogel degradation was first confirmed in acellular hydrogels. Juvenile bovine chondrocytes were encapsulated into the hydrogel and neo-tissue assessed for up to 4 weeks, and analyzed weekly. Standard, destructive assays were conducted to quantify the amount of DNA, sulfated glycosaminoglycans (sGAGs), and total collagen, as well as the spatial distribution of ECM within the constructs. Nondestructive assays were conducted based on mechanical properties and ultrasound measurements. The non-destructive assays were compared to the standard destructive assays to further evaluate their potential in assessing the evolution and quality of the neo-tissue in synthetic degrading hydrogels.

2. Materials and methods

2.1 Materials

Penicillin-Streptomycin (P/S), Fungizone and GlutaGRO™ were from Corning Cellgro (Manassas, VA)[1]. Hoechst 33258 was from Polysciences, Inc. (Warrington, PA). Irgacure 2959 (I2959) was from BASF (Tarrytown, NY). Fetal bovine serum (FBS) was from Atlanta Biologicals (Lawrenceville, GA). Retrievagen A antigen retrieval solution was from BD

---

[1]Certain commercial equipment, instruments, or materials are identified in this paper in order to specify the experimental procedure adequately. Such identification is not intended to imply recommendation or endorsement by the National Institute of Standards and Technology, nor is it intended to imply that the materials or equipment identified are necessarily the best available for the purpose.

Biosciences (San Jose, CA). Keratanase I was from MP Biomedical (Solon, OH). Collagenase type II and papain were from Worthington Biochemical (Lakewood, NJ). Ethyl ether, ethylene diamine tetra acetic acid (EDTA) and Triton X-100 were from Fischer Scientific (Fair Lawn, NJ). The LIVE/DEAD® assay, phosphate-buffered saline (PBS), gentamycin, HEPES buffer, minimal essential medium non-essential amino acids (MEM-NEAA), trypan blue, DAPI, AlexaFluor 488-conjugated goat anti-rabbit IgG and AlexaFluor 546-conjugated goat anti-mouse IgG were from Invitrogen (Carlsbad, CA). PEG (M_W 20 000) was from JenKem Technology USA (Plano, TX). L-proline, L-ascorbic acid, bovine serum albumin (BSA), dimethyl methylene blue (DMMB), ε-Caprolactone, stannous octoate, 5-norbornene-2-carboxylic acid, N,N′-Diisopropylcarbodiimde (DIC), pyridine, 4-(Dimethylamino)pyridine (DMAP), chondroitinase ABC and hyaluronidase were from Sigma-Aldrich (St Louis, MO). Mouse anti-aggrecan antibody (A1059-53E) and rabbit anti-collagen II antibody (C5710-20F) were from US Biologicals (Swampscott, MA). Fluoromount-G® was from SouthernBiotech (Birmingham, AL).

2.2 Macromer synthesis

Macromers of PEG-caprolactone (PEG-CAP) endcapped with norbornene (PEG-CAP-NOR) were synthesized by first reacting 8-arm PEG-hexaglycerol (20 kDa) with ε-caprolactone and stannous octoate as the ring-opening catalyst following protocols adapted from [27]. All reactions were conducted in argon purged reaction vessels unless mentioned otherwise. Briefly, the 8-arm PEG-hexaglycerol was melted at 90 °C and then reacted with 1.5 fold molar excess of ε-caprolactone (per arm of the PEG molecule) in the presence of stannous octoate under vacuum at 140 °C for 6 hours. The PEG-CAP product was purified by precipitation in ice-cold ethyl ether. PEG-CAP was subsequently reacted with 5-norbornene-2-carboxylic acid (10 molar excess), DIC (10 molar excess), DMAP (1 molar excess), pyridine (10 molar excess) in dichloromethane under argon and overnight at room temperature (RT). The final PEG-CAP-NOR product was purified by filtration over active carbon and precipitation in ice-cold ethyl ether. The product was then dried, re-dissolved in a minimum amount of chloroform and further purified by two washes in glycine buffer (0.05 M sodium chloride, 0.05 M sodium hydroxide, 0.05 M glycine) and one wash in brine solution (saturated sodium chloride solution, 36 g per 100 ml). The final product was recovered by precipitation in ice-cold ethyl ether. The final product was confirmed by ^{1}H nuclear magnetic resonance spectroscopy. The number of caprolactones per PEG arm was determined by comparing the area under the integral for the methylene protons (δ=2.25–2.4 ppm) in the caprolactone to the methylene protons (δ=3.25–3.9 ppm) in PEG molecule. The percent norbornene conjugation was determined by comparing the area under the integral for the vinyl protons (δ=5.9–6.25 ppm) to the methylene protons in the PEG molecule. Two 8-arm PEG macromers were synthesized and characterized (Table 1).

2.3 Acellular hydrogel formation

A 10 % w/w macromer solution of PEG-CAP-NOR-I macromer was prepared in PBS + antibiotics. Cylindrical gels (~2mm in height and ~5 mm in diameter) were prepared through photopolymerization with 0.05 % of sterile-filtered photoinitiator I2959 and 1 kDa PEG-dithiol as crosslinker under 352 nm light for 7 minutes. The thiol to ene molar ratio was 1:1. The gels were cultured in 24-well plates with 2 ml of either chondrocyte medium or

chondrocyte medium without addition of serum for up to 4 weeks. The media were changed thrice per week.

2.4 Acellular hydrogel characterization of degradation

PEG-CAP-NOR-I was used for the acellular degradation study. Hydrogels were characterized by a tangent modulus under compression and mass swelling ratio every 2–4 days during degradation (n=2, 10 time-points). For determination of the tangent modulus under compression, hydrogels were compressed to 15 % strain at a rate of 0.5 mm/min using MTS Synergie 100 (10 N load cell). The compressive modulus was calculated from the linear portion of the stress-strain curve between 10 % and 15 % strain. The mass swelling ratio, (q=swollen mass/dry polymer mass), was determined by weighing the swollen mass and weighing the dry polymer mass after lyophilization. The dry mass was corrected to remove the mass contributing from the media and serum.

2.5 Chondrocyte isolation

Full-depth articular cartilage was harvested from the patellar-femoral groove of 1–3 week old calves (Research 87, Marlborough, MA) as previously described [28]. Briefly, cartilage was finely minced, washed in PBS + 1 % P/S + 0.5 μg/ml Fungizone + 20 μg/ml gentamycin (PBS + antibiotics) and digested for 15–17 hours in 560 units/ml Collagenase type II in DMEM + 5 % FBS. The digest was passed through a 100 μm cell strainer. Freshly isolated chondrocytes were washed one time in PBS + antibiotics + 0.02 % EDTA and two times in PBS + antibiotics and re-suspended in chondrocyte medium (DMEM supplemented with 10 % FBS, antibiotics, 0.1 M MEM-NEAA, 0.4 mM L-proline, 50 mg/ml L-ascorbic acid, 4 mM GlutaGRO™, 10 mM HEPES buffer and 110 mg/L sodium pyruvate). Cellular viability of > 90 % was confirmed by trypan exclusion.

2.6 Chondrocyte encapsulation and culture

PEG-CAP-NOR-II was used for all cellular studies. A 3x concentrated cell solution was prepared in PBS + antibiotics to yield a final cell density of 100×10^6 cells/ml. Solutions of photoinitiator and 1kDa PEG-dithiol crosslinker were prepared to yield 0.05 % of sterile photoinitiator I2959 and a thiol to ene molar ratio of 1 to 1. PEG-CAP-NOR-II was re-suspended in PBS + antibiotics, mixed with the sterile photoinitiator and the crosslinker and then mixed with the cell stock to yield a final macromer solution of 10 % w/w. Cubic 5×5×5 mm gels were prepared by photopolymerization as described above. After photopolymerization, gels were briefly washed in PBS + antibiotics to remove any unreacted components. The gels were transferred to 6-well plates with 8 ml of chondrocyte medium per well. The medium was changed thrice weekly. Plates were cultured in a cell culture incubator at 5 % CO_2 and 37 °C.

2.7. Cellular viability

Cellular viability was assessed on half constructs (n=2) using the LIVE/DEAD® assay after 24 hours and 7, 14, 21 and 28 days. Images (3–10 per hydrogel) were taken randomly along the cut side to capture both the interior of the hydrogel and the edge of the hydrogel. Images

were acquired with a laser scanning confocal microscope (Zeiss LSM 510, Thornwood, NY) and a 10× objective.

2.8 Mechanical properties and ultrasound assessment

After 7, 14, 21 and 28 days samples were harvested for simultaneous evaluation of ultrasound and mechanical properties (n=4). A custom-built instrument [22] was used to assess both ultrasound and mechanical properties. For determination of the compressive modulus, hydrogels were compressed at a constant strain rate of 2 mm/min (or 20–25%/min) to a maximum of 1.6 mm. From the stress/strain curve, the secant modulus at 10 % strain was calculated. Ultrasound measurements were performed as described in [22] using a pulse-echo mode to determine the backscatter properties of the constructs. This mode was chosen because previous studies have shown a correlation between backscatter properties and the density of accumulated matrix molecules [26]. In brief, an ultrasound pulse was generated from a commercial pulser/receiver (UTEX 340, Mississauga, Ontario, Canada) and a 100 MHz acoustic transducer (V3346-SU/RM, Olympus, Waltham, MA). The signal passed through the sample in a well and was reflected from the stainless-steel platen, traveling back though the sample. The signal was then digitized (one gigasample/second, 8-bit resolution), using a high-speed digitization card (STR1G Sonix, Sprinfield, VA). The hydrogel was scanned using step sizes of 0.5 mm radially and 0.5 ° circumferentially. The peak amplitude of the largest pulse echo from the platen was determined with the Hilbert transformation using Matlab software (Mathworks, Natick, MA). The amplitude of the signal was influenced by the construct, the medium, the transducer sensitivity and acoustic impedance, which were not separated. However, the effects due to the culture medium, the sensitivity of the transducer, and acoustic impedance are assumed to be the same across all cellular and acellular constructs. The acoustic impedance of fully developed cartilage is about 1.7×10^6 kg $(m^2\ s)^{-1}$ [29], which is close to that of water $(1.5 \times 10^6$ kg $(m^2\ s)^{-1}$). A neo-tissue or acellular scaffold would be in between as seen in results of [26]. Therefore, the net amplitude of the echo from the stainless-steel platen is reported for acellular and cellular hydrogels. Any differences are therefore associated with changes occurring within the hydrogel construct.

2.9 Biochemical analyses

After 7, 14, 21 and 28 days, the same samples that were used to determine the ultrasound and mechanical properties of the constructs, were used for the evaluation of wet weight (n=4) and then harvested for biochemical analyses (n=4). Hydrogel constructs were frozen and stored at −80 °C until further evaluation. For evaluation, hydrogels were homogenized and digested in papain (0.125 mg/ml) for 16 hours at 60 °C. The DNA content was measured using Hoechst 33258 [30]. The amount of sGAGs was measured using the DMMB dye method [31]. The amount of collagen was determined using the hydroxyproline assay under the assumption that collagen has a hydroxyproline content of 10 % [21].

2.10 Immunohistochemical analyses

After 7, 14, 21 and 28 days, half samples were harvested for evaluation for immunohistochemistry (IHC) (n = 2). Constructs were fixed in 4 % paraformaldehyde overnight at 4 °C, transferred to 30 % sucrose overnight at 4 °C, and finally placed in

Tissue-Tek® O.C.T compound (Sakura Finetek USA, Torrance, CA) overnight at RT. The samples were embedded in fresh Tissue-Tek® O.C.T compound and snap-frozen using liquid N_2 and isopentane. Samples were stored at −80 °C until further processing. The samples were prepared such that the sections were obtained from the central region of the hydrogel (i.e., the cut side). Sections (12 μm) were prepared using a Leica CM1850 cryostat (Leica Microsystems Inc., Buffalo Grove, IL). Antibody treatments, enzymatic pre-treatments and image acquisition were conducted as described in [32]. Briefly, sections were subjected to antigen retrieval for aggrecan. Sections were pre-treated for 1 hour at 37 °C with hyaluronidase (200 U) for collagen type II and aggrecan and additionally with chondroitinase ABC (10 mU) and Keratanase I (4 mU) for aggrecan. Sections were treated with primary antibodies at 4°C overnight using a 1 to 5 (aggrecan) or 1 to 50 (collagen type II) dilution. Sections were treated with AlexaFluor 488 (collagen type II) or 546 (aggrecan) conjugated secondary antibodies for 2 hours at RT. Cell nuclei were counterstained with DAPI. Sections that were not exposed to the respective primary antibody served as negative controls. Bovine articular cartilage served as positive controls. Image acquisition was conducted by laser scanning confocal microscopy with a 40× oil objective.

2.11 Statistical analyses

All data are presented as average with one standard deviation. For the acellular studies, two-way analysis of variance (ANOVA) was conducted with time and media condition as factors. For the biochemical content of the construct, the secant modulus and the ultrasonic data, one-way analysis of variance (ANOVA) was conducted with time as the factor. Post-hoc analyses were performed using the Tukey HSD test with $\alpha = 0.05$. The KaleidaGraph software (version 4.1.3) was used. The *p*-values are provided as an indication of significance.

3. Results

3.1 Acellular hydrogel degradation

Degradation of acellular gels, prepared from PEG-CAP-NOR-I batch, was analyzed over the course of 33 days in serum- and serum+_chondrocyte medium. Time was a factor ($p < 0.0001$) in compressive modulus (Fig. 1B) and a factor ($p < 0.0001$) in the mass swelling ratio, q, (Fig. 1C). Serum was a factor ($p = 0.043$) for mass swelling ratio, but less of a factor ($p = 0.12$) for compressive modulus. Over the 33 days, the compressive modulus dropped from ~60 kPa initially to ~9 kPa for the serum-media and to ~3 kPa for the serum+ media condition. The mass swelling ratio increased from ~13 to ~22 for serum-medium condition and from ~13 to ~25 for the serum+ media condition. The hydrogels did not reach reverse gelation by the end of the study at 33 days.

3.2 Cell viability and DNA content

Chondrocytes were encapsulated in hydrogels prepared from the PEG-CAP-NOR-II batch and used for all subsequent experiments. A membrane integrity assay was used to qualitatively assess cell viability and cell distribution within the hydrogel constructs over time. Representative images are shown in Fig. 2A–H. One day after encapsulation (Fig. 2A), the cells were fairly evenly distributed throughout the hydrogel. In addition, the cells were

largely viable with some dead cells present. The latter observation was consistent over the course of the study (Fig. 2B–H). The formation of large cell clusters was visible in some regions of the hydrogel at day 14 (Fig. 2D) and appeared to get larger with culture time (Fig. 2F for day 21, Fig. 2H for day 28). The amount of DNA within the hydrogel constructs increased ($p = 0.0047$) with culture time (Fig. 2I). In particular, DNA content increased ($p = 0.0037$) from days 7 to 14 and then remained relatively constant for the remainder of the experiment.

3.3 Biochemical content

Matrix deposition was assessed by quantifying sGAG content and total collagen content (Fig. 3). The sGAG content within the constructs (Fig. 3A) increased ($p = 0.011$) with culture time. In particular, sGAG increased ($p = 0.029$) by 2.2-fold from days 7 to 14 and then remained relatively constant for the remainder of the experiment. sGAG release to the culture medium was detected. The cumulative sGAG release (Fig. 3B) increased ($p<0.0001$) with culture time and represented ~5 % and 25 % of the total amount of sGAG produced over the course of days 7 and 28, respectively. The total collagen content also increased ($p = 0.00021$) with culture time (Fig. 3C) with a 7-fold increase ($p < 0.0001$) from days 7 to 28. The largest increase ($p = 0.022$) occurred from days 7 to 14 and then only moderately increased each week (e.g., $p = 0.38$ from days 14 to 21, $p = 0.11$ from days 21 to 28).

3.4 Spatial distribution of ECM

To visualize cartilaginous-like matrix production and distribution throughout the constructs, immunohistochemical analyses for aggrecan (Fig. 4) and collagen type II (Fig. 5) were conducted after 7, 14, 21 and 28 days. Aggrecan deposition was located peri-cellularly at day 7 (Fig. 4A). At 14 days (Fig. 4B), aggrecan deposition appeared to increase, but remained located peri-cellularly with some evidence of territorial matrix formation. At day 21 (Fig. 4C) and more so at day 28 (Fig. 4D), the spatial distribution of aggrecan appeared to be greater with the formation of an inter-territorial matrix. The negative control (Fig. 4E) showed no non-specific binding of the secondary antibody. Young bovine knee cartilage was used as positive control (Fig. 4F).

Similar results were observed for collagen type II. At day 7 (Fig. 5A), collagen type II deposition was mainly located peri-cellularly. At day 14 (Fig. 5B), collagen type II deposition increased but remained located peri-cellularly with some evidence of territorial matrix formation. By day 21 (Fig. 5C), the spatial distribution of collagen type II appeared to be greater with the formation of inter-territorial matrix. By day 28 (Fig. 5D), there was abundant collagen type II that appeared to be aligning radially from the cells. The negative control (Fig. 5E) showed no non-specific binding of the secondary antibody. Young bovine articular cartilage was used as positive control (Fig. 5F).

3.5 Nondestructive assessment

The constructs were analyzed by simultaneous assessment of mechanical testing and ultrasound measurements (Fig. 6A). The mechanical properties were assessed by the secant modulus under compression at 10 % strain (Fig. 6B). The secant modulus increased ($p = 0.00018$) with culture time with a 8-fold increase ($p = 0.0002$) from days 7 to 28. There was

no significant increase ($p = 0.95$) in modulus from days 7 to 14. The largest increase ($p = 0.0005$) occurred between days 14 and 28. Cellular constructs were also compared to acellular constructs made from the PEG-CAP-NOR-II batch. The modulus of the cellular constructs was slightly lower ($p = 0.23$ and 0.15, respectively) at days 7 and 14, but by day 21 was higher ($p = 0.085$) when compared to the acellular constructs. For the PEG-CAP-NOR-II batch used in these cellular and acellular experiments, the acellular hydrogels had not yet reached reverse gelation by day 28, but were too difficult to handle to obtain any reliable measurements.

The ultrasonic properties of the acellular and cellular constructs (Fig. 6C–E) were determined by measuring the ultrasound signal as it is goes through the sample, reflected off of the stainless steel sample well, and reflected back through the sample and to the detector. The signal that is measured is defined as the reflection amplitude. Multiple measurements were made across the surface of each hydrogel and are represented in dot plots for all hydrogels for each condition (Fig. 6C). Dot plots for each individual hydrogel construct are provided in supplementary material (Fig. S1). The dot plots illustrate the spatial variation in the ultrasound signal across the hydrogels. The variation was lowest at day 28 for the cellular hydrogels, correlating with the greatest amount of spatially distributed ECM. The measurements across each hydrogel were also averaged to determine a single value and then presented as an average for the different acellular (Fig. 6D) and cellular (Fig. 6E) conditions. The mean reflection amplitude was higher for the acellular constructs than the cellular constructs and was most significant ($p = 0.001$) at day 14. For the cellular constructs the reflection amplitude varied ($p = 0.0012$) with culture time. In particular, the reflection amplitude decreased ($p = 0.012$) between days 7 and 14, increased ($p = 0.002$) between days 14 and 21 to values similar ($p = 0.89$) to that on day 7, and decreased ($p = 0.013$) again between days 21 and day 28.

Plots were also generated to compare the data obtained from the nondestructive measurements (i.e., secant modulus and reflection amplitude of the ultrasound signal) to that of the destructive measurements (i.e., biochemical contents) (Fig. 7). There was no obvious correlation between sGAG and secant modulus (correlation coefficient, $r = 0.51$) (Fig. 7A). A positive correlation between total collagen content and secant modulus was observed (correlation coefficient, $r = 0.83$) (Fig. 7B). For the ultrasound data, there was a general trend showing a decrease in relative reflection amplitude with increasing sGAG content (Fig. 7C) and total collagen content (Fig. 7D) from the initial acellular gel up to day 14, but after which the signal showed no trend.

4. Discussion

This study investigated the use of nondestructive measurements to assess the developing neo-tissue in a new, degradable, and photoclickable PEG hydrogel platform for cartilage TE. Most promising, this hydrogel platform supported juvenile bovine chondrocytes leading to improved neo-tissue deposition with inter-territorial matrix formation and enhanced mechanical properties within four weeks. Nondestructive measurements of the evolving tissue for mechanical and ultrasonic properties yielded information that correlated with not only ECM deposition, but also to spatial distribution. Overall, this new photo-clickable PEG

hydrogel containing caprolactone segments is a promising new synthetic degradable hydrogel for cartilage TE.

A PEG hydrogel formed from step-growth polymerization of thiol-norbornene macromers was modified with caprolactones to introduce hydrolytically labile ester bonds surrounded by a hydrophobic segment. Studies have investigated PEG hydrogels formed from a chain-growth polymerization of polycaprolactone-*b*-PEG-*b*-polycaprolactone dimethacrylate macromers for cartilage TE. Interestingly, these chain-growth hydrogels were relatively stable in aqueous environments, requiring the addition of an enzyme to facilitate degradation [33]. In contrast, the hydrogels employed here were readily degradable in aqueous solutions. This difference is attributed to the accessibility of water molecules to cleave the ester bonds within the hydrophobic caprolactone segments. In chain-growth polymerization, dense hydrophobic regions form [34], which are likely to reduce their availability to water molecules. On the other hand, the step-growth polymerization produces network structures that are more homogenous [35] and therefore more accessible to water molecules and thus hydrolysis. Caprolactones fall into the class of α-hydroxyl esters, which have been shown to also be susceptible to esterases found in serum [36, 37]. In this study, serum had some effect on the degradation behavior of the hydrogel, but was less pronounced than that described for PEG hydrogels formed from chain-growth polymerizations [38]. These findings suggest that the degradation of this step-growth PEG hydrogel modified with caprolactone segments is predominantly controlled by hydrolysis in aqueous solutions.

This hydrolytically degradable step-growth PEG hydrogel supported cartilage-specific ECM deposition with the presence of aggrecan and collagen type II and led to an 8-fold increase in the modulus within four weeks. This finding is a significant improvement over other reports, which employed degradable hydrogels for chondrocyte encapsulation and cartilage TE. For example, a 7-fold decrease in modulus was reported within two weeks of culture and remained low at four weeks for chondrocytes encapsulated in a PEG hydrogel with lactic acid segments formed by chain-growth [14]. Another study reported a 50% lower modulus in degradable PEG hydrogels with caprolactone segments formed by chain growth when compared to non-degradable PEG hydrogels after six to eight weeks of culture [33]. In a more biomimetic hydrogel containing photocrosslinked gelatin and hyaluronic acid, the modulus was reported to increase by ~2.2-fold, but this was over the course of eight weeks [39]. Mathematical models have been used to show the importance of tuning hydrogel degradation with matrix elaboration in order to maintain or achieve increases in the overall modulus [40, 41]. This of course depends on the relative rates of hydrogel degradation and matrix synthesis as well as the concentration of cells in the hydrogel [40, 41]. The promising findings from this study suggest that the degradation behavior of this degradable step-growth PEG hydrogel matches with the ECM synthesis and deposition of the encapsulated cells.

Weekly assessments of the constructs provide insights into the role of hydrogel degradation on the overall neo-tissue development. In particular, the amount of ECM produced and deposited in the hydrogel was greatest in the first two weeks, but the ECM was largely restricted to the peri-cellular space. This observation is indicative of a hydrogel mesh that restricts diffusion of these large ECM molecules [41]. By days 21 and 28, the amount of ECM that was present within the hydrogels appeared to level off, but diffusion of the ECM

molecules into a territorial matrix became evident. This result is only possible with complete degradation of the hydrogel and was most pronounced by day 28, which is consistent with the degradation of the acellular hydrogels occurring predominantly between days 21 and 28. This is also consistent with the observed formation of cell clusters which appeared on day 14 and which can only form once the hydrogel has completely degraded in that region. Interestingly, the modulus was not affected by the initial peri-cellular deposition of ECM during the first two weeks of culture. However, the correlation coefficient between the secant modulus and total collagen content increases from 0.84 to 0.998 if the initial acellular and day 7 time points are excluded. Quantitative evaluation of sGAGs, however, was not sufficient to capture matrix deposition and correlate with modulus. This observation is attributed to the fact that sGAGs can be found in aggrecan aggregates, but also in aggrecan monomers and degraded aggrecan products. While aggrecan aggregates are very large macromolecules with restricted diffusion, aggrecan monomers and degraded aggrecan products are smaller and therefore are more likely to diffuse through the hydrogel. This observation is supported by the detection of sGAGs in the culture medium. As a result, these smaller molecules may not contribute to the deposited matrix and therefore do not contribute to the overall modulus. Nonetheless, the modulus, which can be used as a nondestructive measurement, appears to be closely linked to the evolution of hydrogel degradation and the elaboration of newly deposited ECM containing collagen type II and aggrecan macromolecules.

Ultrasound was used in tandem with mechanical testing as another nondestructive measurement to evaluate the evolution of neo-tissue formation within these degradable PEG hydrogels. Attenuation of the ultrasound signal occurs as the hydrogel transitions from a construct that is predominantly polymer and water to a construct filled with dense ECM [22, 26]. Interestingly, deposition of ECM that was restricted to a peri-cellular matrix was detected by ultrasound, leading to a decrease in the signal from the initial signal in the acellular gels through day 14. This result is supported by previous studies showing attenuation of the ultrasound signal with peri-cellular matrix deposition in non-degrading PEG hydrogels [22]. Over this narrower range, there was a strong negative correlation between the ultrasound signal and sGAG content (r=0.98) and total collagen content (r=0.999). However at day 21, the amount of ECM present began to level off but at the same time there were signs of ECM diffusion as a territorial matrix began to form. These observations correlated with an increase in the ultrasound signal, that is, less ultrasound was scattered away from the receiver. This statement is supported by the fact that ultrasound is reflected at any interface between materials of different mechanical properties or orientations; more randomly oriented interfaces (scatterers) means a reduction in the reflection amplitude [42]. By day 28, a structured matrix was evident which coincided with a second drop in the ultrasound signal (more scatterers). This is observation is consistent with our previous studies showing attenuation of the ultrasound signal after longer (4–9 weeks) *ex vivo* culture times in a chondrocyte-laden degradable hydrogel [26].) There was a ~70% increase in collagen deposition from day 14 to day 28, and at day 28 the histology of collagen type II (Fig. 5 D) appears to show collagen fibers beginning to align radially around each of the cells in contrast to the smooth collagen at day 14 (Fig. 5 C). The radial alignment of the fibers would appear as an anisotropic medium to the propagating ultrasonic wave.

Hall *et al.* [43] have shown that the orientation of a anisotropic ECM increases the apparent scattering. We speculate that this radially aligned collagen would cause more scattering as the ultrasound wave passed through it and consequently the decrease in the ultrasound amplitude at day 28. Interestingly, the variance in the ultrasound signal was also lower at day 28 when compared to day 14, suggesting that the ECM may have been more distributed throughout the hydrogel at the later time point. Taken together, these results support the hypothesis that ultrasound may provide a measurement of ECM structure within the hydrogel and thus may be able to capture changes in the organization of the ECM structure as it develops over time. However, additional studies are needed to test this hypothesis.

Overall, this study investigated two nondestructive measurements based on the secant modulus and the reflection amplitude of an ultrasound signal as it passes through the construct and compared them to two destructive measurements of ECM content and organization. Interestingly, the two nondestructive measurements appear to provide different information regarding the evolution of the neo-tissue. Taken together, we summarize our interpretation of the two nondestructive measurements as follows and put forth a new hypothesis. An attenuation in the ultrasound signal concomitant with no change in the secant modulus suggests the formation of a peri-cellular matrix with little to no change in the hydrogel properties as a result of hydrogel degradation. An increase in the secant modulus concomitant with an increase in the ultrasound signal suggests the beginning of ECM diffusion and territorial matrix formation with hydrogel degradation, but with minimal additional deposition of ECM. Finally, further increases in the secant modulus concomitant with an attenuation of the ultrasound signal is coupled with additional ECM production and deposition. Therefore, the combination of these two nondestructive measurements may provide important information regarding ECM deposition, evolution, and structure, but additional studies are needed to confirm this connection.

There are several limitations of this study. Most notably, juvenile bovine chondrocytes were used as a model cell type, which have been shown to have a higher anabolic activity and lower catabolic activity when compared to bovine chondrocytes isolated from older donors [44, 45] and therefore may not be representative of the more clinically relevant human chondrocytes. Nonetheless, this model cell type enables us to establish a better understanding of the connection between hydrogel degradation and ECM synthesis and deposition. This information can then be used in the future to aid in hydrogel designs with hydrogel degradation profiles that match ECM synthesis and deposition for different cell sources [41]. A second limitation of the study is the relatively short culture time of four weeks. Although the modulus increased by 8-fold over this relatively short period of time, the modulus of the engineered tissue is lower than that of bovine articular cartilage by nearly two orders of magnitude [46]. Longer culture times combined with mechanical loading may lead to improved mechanics that approach that of native tissue [47] and is a focus of future studies. A third limitation of this study is that ECM assessment was limited to aggrecan and collagen type II, but it is well known that crosslinking of collagen fibers can lead to improvements in mechanical properties without the addition of new matrix [48]. A final limitation of this study is that ultrasound measurements were limited to the attenuation of the ultrasound signal (i.e., backscatter properties). Other studies have shown a strong correlation with speed of sound and the modulus of hydrogel materials [23] and cartilage

[25] and therefore future studies should incorporate both backscatter and speed of sound measurements.

5. Conclusion

Photo-clickable and hydrolytically degradable PEG hydrogels containing caprolactone segments were established as a promising platform for cartilage TE by maintaining viable chondrocytes, supporting cartilage-specific ECM deposition, and most excitingly resulting in an ~8-fold increase in mechanical properties. In addition, the utility of nondestructive measurements based on mechanical and ultrasound properties were demonstrated. These measurements seem to provide information beyond simple quantitative measures of total amounts of ECM and may provide additional information regarding the formation of a territorial matrix and matrix structure, both of which are ultimately critical to using an engineered tissue to restore mechanical function to the damaged tissue. However, further studies are needed to establish the long-term relationship between mechanical properties and ultrasound measurements and the quality of the developing engineered cartilage tissue.

Supplementary Material

Refer to Web version on PubMed Central for supplementary material.

Acknowledgments

References

1. Buckwalter JA, Mankin HJ. Articular cartilage repair and transplantation. Arthritis & Rheumatology. 1998; 41:1331–42.

2. Madry H, Grun UW, Knutsen G. Cartilage repair and joint preservation: medical and surgical treatment options. Dtsch Arztebl Int. 2011; 108:669–77. [PubMed: 22114626]

3. Reginster JY. The prevalence and burden of arthritis. Rheumatology. 2002; 41(Supp 1):3–6. [PubMed: 12173279]

4. Steadman JR, Rodkey WG, Briggs KK. Microfracture to treat full-thickness chondral defects: surgical technique, rehabilitation, and outcomes. J Knee Surg. 2002; 15:170–6. [PubMed: 12152979]

5. Szerb I, Hangody L, Duska Z, Kaposi NP. Mosaicplasty: long-term follow-up. Bull Hosp Jt Dis Instead of Bulletin. 2005; 63:54–62.

6. Brittberg M, Lindahl A, Nilsson A, Ohlsson C, Isaksson O, Peterson L. Treatment of deep cartilage defects in the knee with autologous chondrocyte transplantation. N Engl J Med. 1994; 331:879–95. [PubMed: 8078542]

7. Gobbi A, Nunag P, Malinowski K. Treatment of full thickness chondral lesions of the knee with microfracture in a group of athletes. Knee Surg Sports Traumatol Arthrosc. 2005; 13:213–21. [PubMed: 15146311]

8. Roberts JJ, Bryant SJ. Comparison of photopolymerizable thiol-ene PEG and acrylate-based PEG hydrogels for cartilage development. Biomaterials. 2013; 34:9969–79. [PubMed: 24060418]

9. Bryant SJ, Anseth KS. Controlling the spatial distribution of ECM components in degradable PEG hydrogels for tissue engineering cartilage. J Biomed Mater Res. 2003; 64A:70–9.

10. Temenoff JS, Athanasiou KA, LeBaron RG, Mikos AG. Effect of poly(ethylene glycol) molecular weight on tensile and swelling properties of oligo(poly(ethylene glycol) fumarate) hydrogels for cartilage tissue engineering. J Biomed Mater Res. 2002; 59:429–37. [PubMed: 11774300]

11. Elisseeff J, Anseth K, Sims D, McIntosh W, Randolph M, Langer R. Transdermal photopolymerization for minimally invasive implantation. Proc Natl Acad Sci U S A. 1999; 96:3104–7. [PubMed: 10077644]

12. Nicodemus GD, Skaalure SC, Bryant SJ. Gel structure has an impact on pericellular and extracellular matrix deposition, which subsequently alters metabolic activities in chondrocyte-laden PEG hydrogels. Acta Biomater. 2011; 7:492–504. [PubMed: 20804868]

13. Bryant SJ, Anseth KS. Hydrogel properties influence ECM production by chondrocytes photoencapsulated in poly(ethylene glycol) hydrogels. J Biomed Mater Res. 2002; 59:63–72. [PubMed: 11745538]

14. Roberts JJ, Nicodemus GD, Greenwald EC, Bryant SJ. Degradation Improves Tissue Formation in (Un)Loaded Chondrocyte-laden Hydrogels. Clin Orthop Relat Res. 2011; 469:2725–34. [PubMed: 21347817]

15. Fairbanks BD, Schwartz MP, Halevi AE, Nuttelman CR, Bowman CN, Anseth KS. A Versatile Synthetic Extracellular Matrix Mimic via Thiol-Norbornene Photopolymerization. Adv Mater (Weinheim, Ger). 2009; 21:5005–10.

16. Metters AT, Anseth KS, Bowman CN. Fundamental studies of a novel, biodegradable PEG-b-PLA hydrogel. Polymer. 2000; 41:3993–4004.

17. Sawhney AS, Pathak CP, Hubbell JA. Bioerodible hydrogels based on photopolymerized poly(ethylene glycol)-co-poly(alpha-hydroxy acid) diacrylate macromers. Macromolecules. 1993; 26:581–7.

18. Tsuji H, Ikada Y. Blends of aliphatic polyesters. 2. Hydrolysis of solution-cast blends from poly(L-lactide) and poly(epsilon-caprolactone) in phosphate-buffered solution. J Appl Polym Sci. 1998; 67:405–15.

19. Farndale RW, Buttle DJ, Barrett AJ. Improved quantitation and discrimination of sulfated glycosaminoglycans by use of dimethylmethylene blue. Biochim Biophys Acta. 1986; 883:173–7. [PubMed: 3091074]

20. Labarca C, Paigen K. A simple, rapid, and sensitive DNA assay procedure. Anal Biochem. 1980; 102:344–52. [PubMed: 6158890]

21. Woessner JF. The determination of hydroxyproline in tissue and protein samples containing small proportions of this imino acid. Arch Biochem Biophys. 1961; 93:440–7. [PubMed: 13786180]

22. Popp JR, Roberts JJ, Gallagher DV, Anseth KS, Bryant SJ, Quinn TP. An instrumented bioreactor for mechanical stimulation and real-time, nondestructive evaluation of engineering cartilage tissue. Journal of Medical Devices. 2012; 6:1–7.

23. Walker JM, Myers AM, Schluchter MD, Goldberg VM, Caplan AI, Berilla JA, Mansour JM, Welter JF. Nondestructive Evaluation of Hydrogel Mechanical Properties Using Ultrasound. Ann Biomed Eng. 2011; 39:2521–30. [PubMed: 21773854]

24. Aula AS, Töyräs J, Tiitu V, Jurvelin JS. Simultaneous ultrasound measurement of articular cartilage and subchondral bone. Osteoarthritis Cartilage. 2010; 18:1570–6. [PubMed: 20950692]

25. Sun A, Bai X, Ju B-F. A new method for evaluating the degeneration of articular cartilage using pulse-echo ultrasound. Rev Sci Instrum. 2015:86.

26. Rice MA, Waters KR, Anseth KS. Ultrasound monitoring of cartilaginous matrix evolution in degradable PEG hydrogels. Acta Biomater. 2009; 5:152–61. [PubMed: 18793879]

27. Bryant SJ, Cuy JL, Hauch KD, Ratner BD. Photo-patterning of porous hydrogels for tissue engineering. Biomaterials. 2007; 28:2978–86. [PubMed: 17397918]

28. Nicodemus GD, Bryant SJ. The role of hydrogel structure and dynamic loading on chondrocyte gene expression and matrix formation. J Biomech. 2008; 41:1528–36. [PubMed: 18417139]

29. Toyras J, Nieminen HJ, Laasanen MS, Nieminen MT, Korhonen RK, Rieppo J, Hirvonen J, Helminen HJ, Jurvelin JS. Ultrasonic characterization of articular cartilage. Biorheology. 2002; 39:161–9. [PubMed: 12082279]

30. Kim YJ, Sah RL, Doong JY, Grodzinsky AJ. Fluorometric assay of DNA in cartilage explants using Hoechst 33258. Anal Biochem. 1988; 174:168–76. [PubMed: 2464289]

31. Templeton DM. The basis and applicability of the dimethylmethylene blue binding assay for sulfated glycosaminoglycans. Connect Tissue Res. 1988; 17:23–32. [PubMed: 3133157]

32. Skaalure SC, Dimson SO, Pennington AM, Bryant SJ. Semi-interpenetrating networks of hyaluronic acid in degradable PEG hydrogels for cartilage tissue engineering. Acta Biomater. 2014; 10:3409–20. [PubMed: 24769116]

33. Rice MA, Anseth KS. Controlling cartilaginous matrix evolution in hydrogels with degradation triggered by exogenous addition of an enzyme. Tissue Eng. 2007; 13:683–91. [PubMed: 17266401]

34. Lin-Gibson S, Jones RL, Washburn NR, Horkay F. Structure-property relationships of photopolymerizable poly(ethylene glycol) dimethacrylate hydrogels. Macromolecules. 2005; 38:2897–902.

35. Hoyle CE, Bowman CN. Thiol-Ene Click Chemistry. Angewandte Chemie-International Edition. 2010; 49:1540–73.

36. Kurono Y, Maki T, Yotsuyanagi T, Ikeda K. Esterase-Like Activity of Human-Serum Albumin - Structure- Activity-Relationships For the Reactions With Phenyl Acetates and Para-Nitrophenyl Esters. Chem Pharm Bull. 1979; 27:2781–6. [PubMed: 527146]

37. Catiker E, Gumusderelioglu M, Guner A. Degradation of PLA, PLGA homo- and copolymers in the presence of serum albumin: a spectroscopic investigation. Polym Int. 2000; 49:728–34.

38. Martens PJ, Bryant SJ, Anseth KS. Tailoring the Degradation of Hydrogels Formed from Multivinyl Poly(ethylene glycol) and Poly(vinyl alcohol) Macromers for Cartilage Tissue Engineering. Biomacromolecules. 2003; 4:283–92. [PubMed: 12625723]

39. Levett PA, Hutmacher DW, Malda J, Klein TJ. Hyaluronic Acid Enhances the Mechanical Properties of Tissue-Engineered Cartilage Constructs. PLoS ONE. 2014:9.

40. Dhote V, Vernerey FJ. Mathematical model of the role of degradation on matrix development in hydrogel scaffold. Biomech Model Mechanobiol. 2014; 13:167–83. [PubMed: 23636471]

41. Dhote V, Skaalure SC, Akalp U, Roberts JJ, Bryant SJ, Vernerey FJ. On the role of hydrogel structure and degradation in controlling the transport of cell-secreted matrix molecules for engineered cartilage. J Mech Behav Biomed Mater. 2013; 19:61–74. [PubMed: 23276516]

42. Chan, V.; Perlas, A. Basics of Ultrasonic Imaging. In: Narouze, SN., editor. Atlas of Ultrasound Guided Procedures in Interventional Pain Management. Springer; 2011.

43. Hall CS, Scott MJ, Lanza GM, Miller JG, Wickline SA. The extracellular matrix is an important source of ultrasound backscatter from myocardium. J Acoust Soc Am. 2000; 107:612–9. [PubMed: 10641669]

44. Skaalure SC, Milligan IL, Bryant SJ. Age impacts extracellular matrix metabolism in chondrocytes encapsulated in degradable hydrogels. Biomedical Materials. 2012:7.

45. Farnsworth N, Antunez LR, Bryant SJ. Dynamic Compressive Loading Differentially Regulates Chondrocyte Anabolic and Catabolic Activity with Age. Biotechnol Bioeng. 2013; 110:2046–57. [PubMed: 23404228]

46. Aspden RM, Larsson T, Svensson R, Heinegard D. Computer-controlled mechanical testing machine for small samples of biological viscoelastic materials. J Biomed Eng. 1991; 13:521–5. [PubMed: 1770815]

47. Mauck RL, Soltz MA, Wang CCB, Wong DD, Chao PHG, Valhmu WB, Hung CT, Ateshian GA. Functional tissue engineering of articular cartilage through dynamic loading of chondrocyte-seeded agarose gels. J Biomech Eng. 2000; 122:252–60. [PubMed: 10923293]

48. Makris EA, Responte DJ, Paschos NK, Hu JC, Athanasiou KA. Developing functional musculoskeletal tissues through hypoxia and lysyl oxidase-induced collagen cross-linking. Proc Natl Acad Sci U S A. 2014; 111:E4832–E41. [PubMed: 25349395]

Statement of Significance

Designing synthetic hydrogels whose degradation matches tissue growth is critical to maintaining mechanical integrity as the hydrogel degrades and new tissue forms, but is challenging due to the nature of the hydrogel crosslinks that inhibit diffusion of tissue matrix molecules. This study details a promising, new, photo-clickable and synthetic hydrogel whose degradation supports cartilaginous tissue matrix growth leading to the formation of a territorial matrix, concomitant with an increase in mechanical properties. Nondestructive assays based on mechanical and ultrasonic properties were also investigated using a novel instrument and found to correlate with matrix deposition and evolution. In sum, this study presents a new hydrogel platform combined with nondestructive assessments, which together have potential for *in vitro* cartilage tissue engineering.
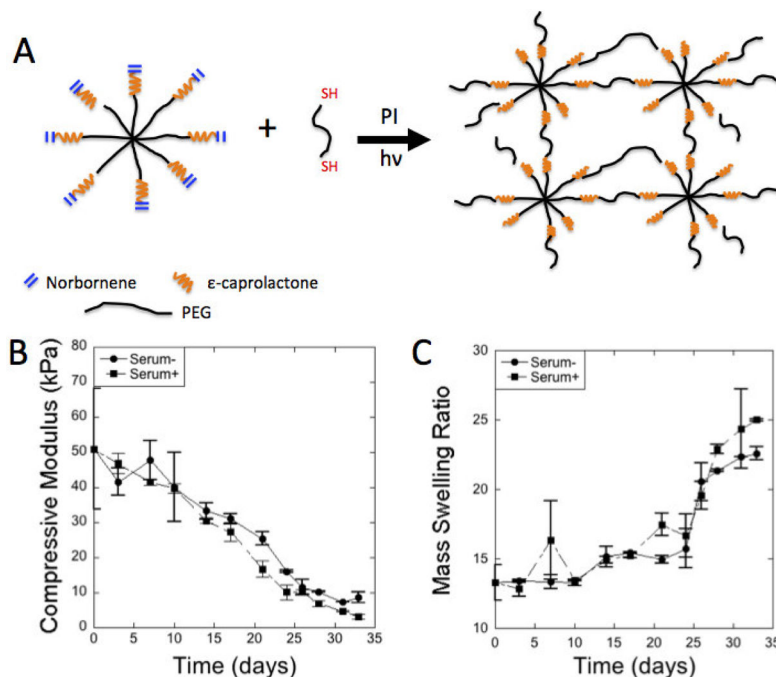
Figure 1.
(A) Schematic of hydrogel formation by a step-growth photo-clickable reaction from macromers of 8-arm PEG-caprolactone functionalized with norbornenes and PEG dithiol crosslinker in the presence of a photoinitiator (PI) and ultraviolet light (hv). (B) Compressive modulus as a function of time for hydrogels prepared from PEG-CAP-NOR-II (n=2–3). (C) Mass swelling ratio (q) as a function of time for hydrogels prepared from PEG-CAP-NOR-II (n=2–3). Acellular hydrogels were placed in either serum-free or serum-plus media.
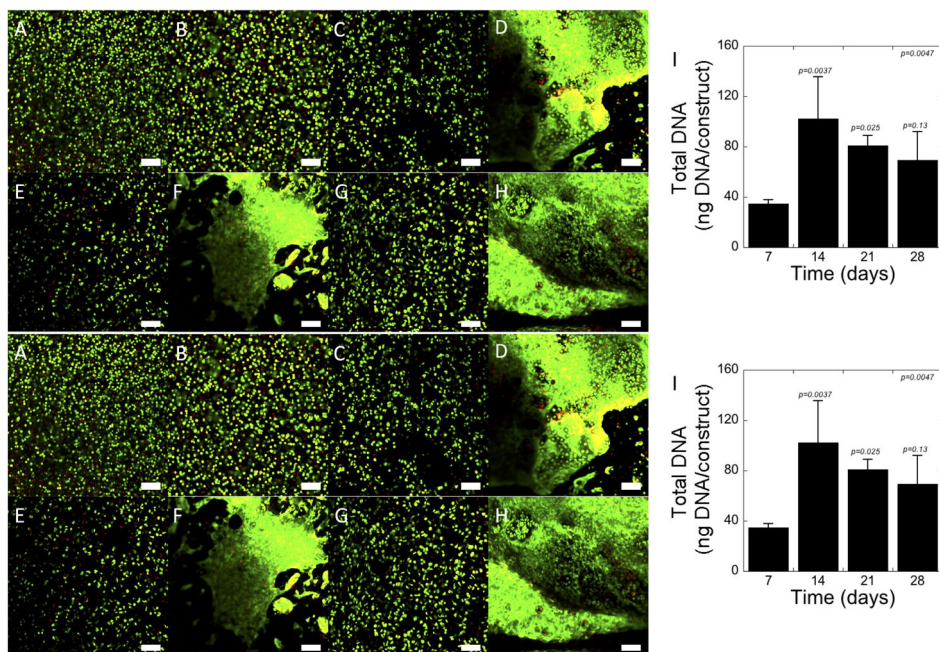
Figure 2.
Cellular viability and DNA content of photo-clickable and degradable PEG hydrogels with encapsulated chondrocytes. LIVE/DEAD® images were acquired at day 1 (A), day 7 (B), day 14 (C,D), day 21 (E, F) and day 28 (G, H). Live cells were stained green with calcein AM and dead cells were stained red with ethidium homodimer. Scale bars indicate 100 μm. The DNA content (I), an indicator for total cell number, was measured at day 7, 14, 21 and 28. p-values are reported for one-way ANOVA ($\alpha=0.05$) in the upper corner with time as the factor. p-values above each column indicate significance compared to day 7. Data are presented as mean with standard deviation as error bars, n=3–4.
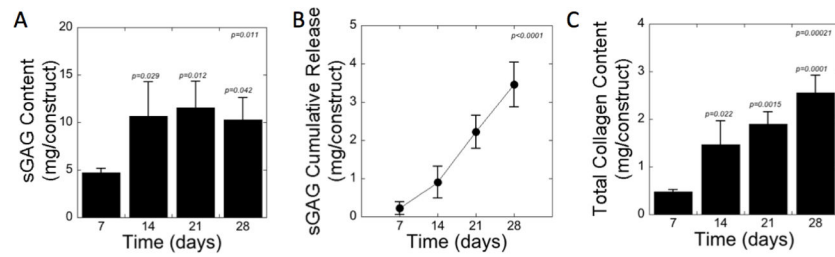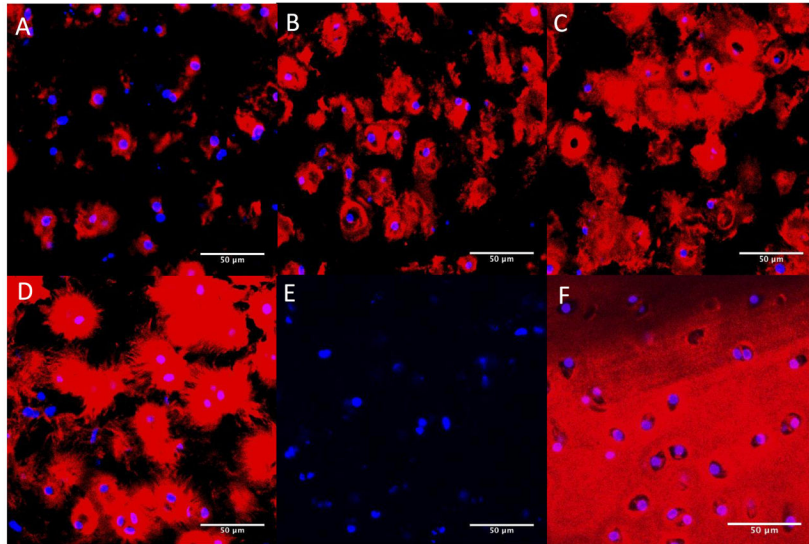
Figure 3.
Biochemical assessment of photo-clickable and degradable PEG hydrogels with encapsulated chondrocytes for (A) sGAG content within the constructs, (B) sGAG cumulative release to the culture medium, and (C) total collagen content within the constructs. *p*-values are reported for one-way ANOVA (α=0.05) in the upper corner with time as the factor. *p*-values above each column in panel A and C indicate significance compared to day 7. Data are presented as mean with standard deviation as error bars, n=3–4.

Figure 4.
Immunohistochemical detection for aggrecan (red) within the photo-clickable and degradable PEG hydrogels with encapsulated chondrocytes after day 7 (A), day 14 (B), day 21 (C) and day 28 (D) of culture. The negative control (E) showed no non-specific staining of the secondary antibody. Bovine articular cartilage was used as positive control (F). Cell nuclei were counterstained with DAPI (blue). All images were taken at 400× magnification; scale bars indicate 50 μm.
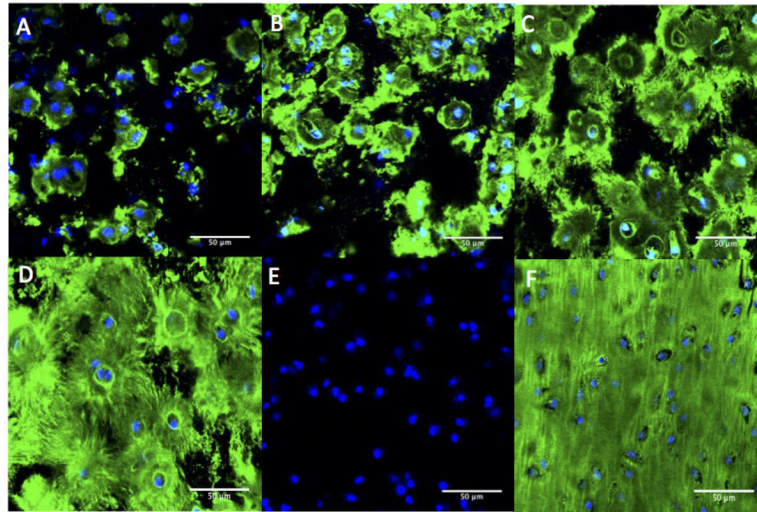
Figure 5.
Immunohistochemical detection for collagen type II (green) within the photo-clickable and degradable PEG hydrogels with encapsulated chondrocytes after day 7 (A), day 14 (B), day 21 (C) and day 28 (D) of culture. The negative control (E) showed no non-specific staining of the secondary antibody. Bovine articular cartilage was used as positive control (F). Cell nuclei were counterstained with DAPI (blue). All images were taken at 400× magnification; scale bars indicate 50 μm.
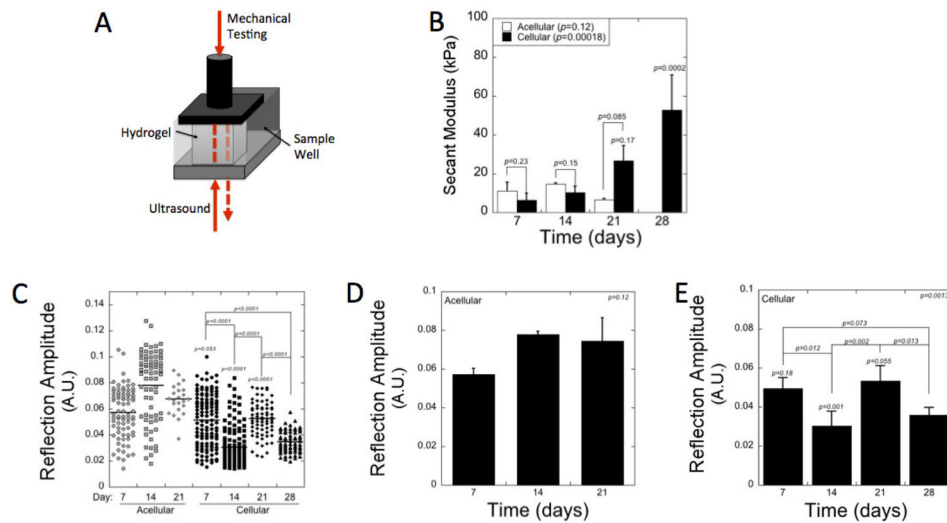
Figure 6.
Nondestructive measurements of photo-clickable and degradable PEG hydrogels with encapsulated chondrocytes using a novel instrument [22] whereby each construct within a sample well shown in (A) can be measured by compression tests and ultrasound signals. (B) The secant modulus at 10% strain was measured as a function of time for acellular (white) and cellular (black) constructs. (C–E) Reflection amplitude of the ultrasound signal was measured after the signal passes through the sample and is reflected back through the sample to the detector. Reflection amplitude measurements were recorded at different locations within each hydrogel specimen and for two to four hydrogel specimen per condition and the data collected are shown as a dot plot in (C), where each symbol represents a unique measurement. The averaged data are shown in (D) and (E) for acellular and cellular constructs, respectively. In B, D, and E, data are presented as mean with standard deviation across the data set for each day as error bars, n=2 for acellular gels and n=3–4 for cellular gels. *p*-values above each column in panel B, D and E indicate significance compared to day 7. *p*-values are reported for one-way ANOVA (α=0.05) in the upper corner of panels B, D, and E with time as the factor. *p*-values are also reported and bars indicate the comparison.
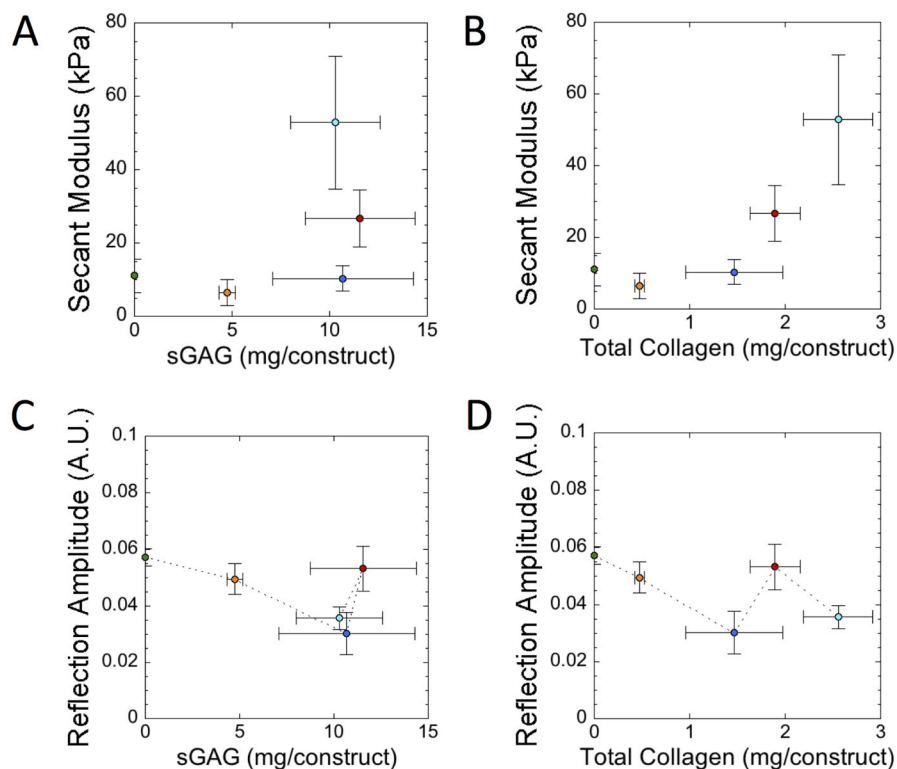
Figure 7.
Scatter plots of (A) secant modulus at 10% strain plotted against sGAG content, (B) secant modulus at 10% strain plotted against total collagen content, (C) reflection amplitude of the ultrasound signal plotted against sGAG content, and (D) reflection amplitude of the ultrasound signal plotted against total collagen content for the photo-clickable and degradable PEG hydrogels with encapsulated chondrocytes over the four week culture period. The data points are color coded each corresponding to a specific time point. The green circle at the '0' condition represents the acellular hydrogel at day 7 containing 0 mg sGAG/construct and 0 mg total collagen/construct. Orange represents day 7, dark blue represents day 14, red represents day 21 and light blue represents day 28. Data are presented as mean with standard deviation as error bars, n=2 for acellular gels and n=3–4 for cellular gels.

Table 1

Multi-arm PEG macromers used in this study

Name	Average Number of Caprolactone Repeat Units per PEG arm	Norbornene Functionalization
PEG-CAP-NOR-I	1.29	65%
PEG-CAP-NOR-II	0.93	75%